

Image-potential states on dielectric-covered metal surfaces: Variational versus numerical approach

B. Trninić-Radja* and M. Šunjić

Department of Physics, University of Zagreb, P.O. Box 162, 41001 Zagreb, Croatia, Yugoslavia

Z. Lenac

Pedagogical Faculty, 51000 Rijeka, Croatia, Yugoslavia

(Received 21 March 1989)

We find a set of simple variational hydrogeniclike wave functions for the three lowest image-potential states of electrons trapped on dielectric layers supported by a metallic substrate. We calculate the variational parameters and find excellent agreement with the numerical calculations, both for eigenenergies and eigenfunctions. A simple form of the wave functions and their accuracy enable analytical formulation and treatment of many-body processes in these quasi-two-dimensional electronic systems.

INTRODUCTION

Many transition-metal surfaces support unoccupied electronic surface states and image-potential states, the latter arising from the attractive long-range electrostatic potential. The existence of these localized states is possible in a gap in the surface-projected bulk density of states, which indicates that the lattice provides a strong repulsive potential in this energy region. In the past decade the observation of these states, using the techniques of optical absorption, inverse photoemission, and electron-energy-loss spectroscopy (EELS), has led to intensified theoretical studies of these phenomena.¹⁻³

These (high-resolution) experimental techniques can be also used to study image-potential states on dielectric surfaces, like liquid He, where they were first predicted⁴ and observed,⁵ and dielectric-covered metal surfaces.^{6,7} In general, one can distinguish between two classes of surface states: the lowest—or “crystal induced”—state is localized in the surface region, its character is determined by the scattering on atomic core potentials, and it is only weakly influenced by the long-range image potential. In fact, it can exist even in the models which assume a sharp surface-potential step. On the other hand, proper image-potential states extend far outside the solid, are given to a good approximation by the solutions of the classical image potential with an infinite repulsive barrier, and are only weakly influenced by the surface scattering. In this respect, they form a model system of a two-dimensional electron gas similar to the electrons adsorbed on liquid helium.^{4,5} However, we are not aware of any systematic experimental study of these states for finite layer thicknesses and different substrates.

The aim of this paper is, therefore, to find simple and accurate analytic forms of wave functions of electrons in image-potential states on dielectric-covered metal surfaces. Using a one-dimensional model of the electrostatic attractive potential, Cole⁸ has calculated numerically the eigenvalues and eigenfunctions of electrons in an image-potential state on a layer of dielectric (H₂, He, Ne) deposit-

ed on a metallic substrate. However, for application in further theoretical work, numerical wave functions are not very useful.

In this paper we suggest variational solutions for the three lowest bound states in the image potential of the dielectric-metal system and evaluate their energies, wave functions, and mean positions. We also calculate numerically the wave functions and energies and compare with the variational results, for three inert dielectrics: liquid He, solid Ne, and Ar.

The simplicity (analytic form) and high accuracy of these variational wave functions make possible the studies of the many-body effects in the quasi-two-dimensional systems of electrons trapped in image-potential states.⁹ The spatial extension of these states changes the form of the effective electron-electron interaction and modifies the phase diagrams for the formation of a two-dimensional Wigner lattice. At higher densities, the self-consistent variational calculations should also include this electron-electron interaction. It turns out¹⁰ that our variational trial functions are still a good starting point, and the results of the present work are quantitatively modified only for the case of helium, i.e., the weakest image potential, at (unphysically) high densities.

FORMULATION OF THE PROBLEM

Figure 1 shows the geometry of the system. A smooth layer of dielectric of thickness d with the static dielectric constant ϵ_0 is deposited on a (metal or dielectric) substrate. The electrons above the dielectric move freely parallel to the surface, and in the perpendicular direction they experience the attractive electrostatic potential and the repulsive exchange potential of atomic closed shells. These two potentials can trap electrons in a series of Rydberg-like bound states that we are going to study in this paper.

In order to determine the electrostatic potential we start with the screened (nonlocal) Coulomb interaction

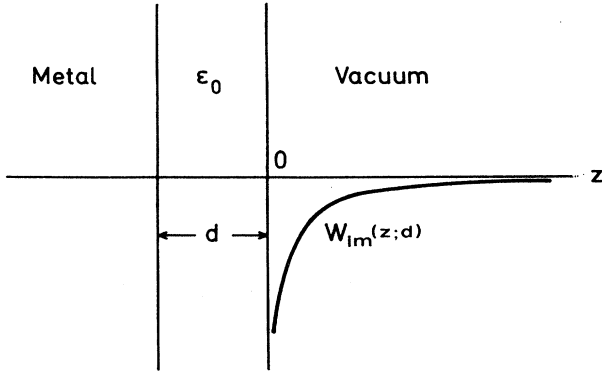


FIG. 1. Geometry of the system: layer of dielectric ($-d < z < 0$) on a metal substrate ($z < -d$). $W_{\text{im}}(z;d)$ is image potential of this system for $z > 0$.

which can be written outside a planar surface for $z, z' > 0$ in the form^{8,11}

$$W(\mathbf{R}, z, z') = \int \frac{d\mathbf{Q}}{(2\pi)^2} e^{i\mathbf{Q}\cdot\mathbf{R}} \frac{2\pi e^2}{Q} \times [e^{-Q|z-z'|} - D(Q, \omega)e^{-Q(z+z')}] . \quad (1)$$

Here, the first term in the square brackets represents the direct interaction, and the second is the induced interaction mediated via the exchange of polarization fluctuations in the solid surface plasmons in a metal, or modified surface excitations in the metal-dielectric system.

For the static problems we can use the high-frequency (instantaneous) limit of $D(Q, \omega)$; furthermore, we shall take a small- Q limit because all the lengths in the problem will be larger than k_F^{-1} or k_{TF}^{-1} where dispersion of surface plasmons starts playing a role.

In this limit, for the layer of an inert dielectric (ϵ_0) of thickness d on a metallic substrate ($\epsilon \rightarrow \infty$), D can be expressed as^{8,12}

$$D(Q) = \frac{\beta + e^{-2Qd}}{1 + \beta e^{-2Qd}} , \quad (2)$$

where

$$\beta = \frac{\epsilon_0 - 1}{\epsilon_0 + 1} . \quad (3)$$

For a clean metal ($d \rightarrow 0$) $D \rightarrow 1$, and for a thick dielectric ($d \rightarrow \infty$) $D \rightarrow \beta$, as expected.

The image potential of the electron corresponds to the local limit ($\mathbf{R} \rightarrow 0, z = z'$) of the electron self-energy derived from the second (induced) terms in (1):

$$\begin{aligned} W_{\text{im}}(x;d) &= \frac{1}{2} \int \frac{dQ}{(2\pi)^2} W_{\text{ind}}(Q, z = z') \\ &= -\frac{e^2}{2} \int dQ e^{-2Qz} D(Q) . \end{aligned} \quad (4)$$

Both for a very thin and very thick layer, the potential reduces to the well-known expression

$$W_{\text{im}}(z;d) = -Z \frac{e^2}{4z} \text{ where } Z \equiv Z(d) \rightarrow \begin{cases} 1 & \text{for } d \rightarrow 0 \\ \beta & \text{for } d \rightarrow \infty \end{cases} , \quad (5)$$

but in the intermediate considered here, case W_{im} is somewhere in between and has to be evaluated from (4). Needless to say, approximating a dielectric layer with a slab of a dielectric constant ϵ_0 appropriate to the bulk dielectric is not valid for very thin layers.

Inserting (2) for $D(Q)$ into (4) leads to a series of images which can be written in a fast-converging form:

$$\begin{aligned} W_{\text{im}} &= -\frac{e^2}{4} \left[\frac{1}{z+d} + \beta \left[\frac{1}{z} - \frac{1}{z+2d} \right] \right] \\ &+ \sum_{n=1}^{\infty} (-1)^n \beta^{n+1} \left[\frac{1}{z+nd} - \frac{1}{z+(n+2)d} \right] . \end{aligned} \quad (6)$$

Here the $(z+d)^{-1}$ and β/z terms are due to the images in the metal and dielectric, respectively, and the other terms are their higher-order images.

ONE-PARAMETER VARIATIONAL WAVE FUNCTIONS

Assuming a strong repulsive barrier at the surface of a dielectric ($z=0$) and the attractive electrostatic potential (4), the eigenstates can be easily calculated in the limiting cases $d=0$ and $d=\infty$, where the potential reduces to the limiting form (5). The wave functions are⁴

$$|\mathbf{K}, \alpha\rangle = e^{i\mathbf{K}\cdot\mathbf{R}} |\alpha\rangle, \quad \mathbf{K} \equiv \mathbf{K}_{\parallel} \quad (7)$$

where the ground-state wave function $|\alpha\rangle$ is of the Rydberg type:

$$\phi_0(z) = |\alpha\rangle = 2\alpha^{3/2} z e^{-\alpha z}, \quad z \geq 0 \quad (8)$$

and the energy (in Ry) of the ground state is

$$E_0(\mathbf{K}) = \frac{\hbar^2 \mathbf{K}^2}{2m} + E_0, \quad E_0 = -\frac{\hbar^2}{2m} \alpha^2 = -\frac{1}{16} \kappa^2, \quad (9)$$

where $\alpha = \kappa/4a_0$. The parameter κ equals 1 for $d=0$ and β for $d=\infty$. For the finite dielectric thickness d , i.e., for the potential (4), Cole⁸ found the eigenenergies E_0 numerically.

For a finite layer thickness d , in analogy with the asymptotic ($d=0$ or ∞) solutions (8) (and corresponding wave functions for higher Rydberg states), we assume the following variational wave functions.

(i) Ground state:

$$\psi_0 = \frac{1}{N_0} \rho e^{-\alpha_0 \rho/4}, \quad N_0^2 = 16a_0/\alpha_0^3 . \quad (10a)$$

(ii) First excited state:

$$\psi_1 = \frac{1}{N_1} (a_1 \rho + a_2 \alpha_1 \rho^2) e^{-\alpha_1 \rho/8}, \quad N_1^2 = 128a_0/\alpha_1^3 . \quad (10b)$$

(iii) Second excited state:

$$\psi_2 = \frac{1}{N_2} (b_1 \rho + b_2 \alpha_2 \rho^2 + b_3 \alpha_2^2 \rho^3) e^{-\alpha_2 \rho / 12},$$

$$N_2^2 = 432 a_0 / \alpha_2^3, \quad (10c)$$

where $\rho = z/a_0$.

The orthonormalization conditions

$$\langle \psi_i | \psi_j \rangle = \delta_{ij} \quad (11)$$

give five relations which determine a 's and b 's as functions of the variational parameters α_0 , α_1 , and α_2 for each thickness d .

The average value $E_i = \langle \psi_i | H | \psi_i \rangle$ of the Hamiltonian

$$H = \frac{\hbar^2}{2m} \frac{d^2}{dz^2} + W_{\text{im}}(z; d) \quad (12)$$

is minimized by requiring

$$\frac{\partial E_i}{\partial \alpha_i} = 0, \quad (13)$$

which gives the values of $\alpha_0 = \alpha_0(d)$, and also the relations

$$\alpha_1 = \alpha_1(\alpha_0, d),$$

$$\alpha_2 = \alpha_2(\alpha_1, \alpha_0, d). \quad (14)$$

These α 's finally determine the wave functions ψ_i and eigenenergies E_i of the three lowest levels. (See Appendix.)

The numerical solutions of the Schrödinger equation are obtained in the standard way, and we might only mention the appropriate boundary conditions. For $\rho \rightarrow 0$, $W_{\text{im}} \rightarrow -e^2 \beta / 4z$, so the wave functions are hydrogenlike wave functions (10) of the form $\psi(\beta \rho)$. For $\rho \rightarrow \infty$, $W_{\text{im}} \rightarrow -e^2 / 4(z+d)$, so the wave functions approach the hydrogenlike wave function (10) shifted by d : $\psi(\rho + d/a_0)$.

DISCUSSION OF THE RESULTS

Figure 2 shows the variationally calculated energies of the ground and first excited states of the three rare-gas layers as functions of the layer thickness.

The (bulk) values of $\epsilon_0 = 1.055$ for He, 1.24 for Ne, and 1.66 for Ar are taken from Ref. 13. The repulsive potential at the dielectric surface, as mentioned earlier, arises from the large gap between the filled and lowest empty bands of the rare-gas solids. In the case of Xe and Kr the hybridization lowers the bottom of the s band below vacuum in a three-dimensional solid, but not necessarily in a layer. For the three gases considered, they are well above the vacuum level.¹⁴⁻¹⁶

If we now calculate numerically these eigenvalues and plot them in Fig. 2, it is almost impossible to resolve them from the variational results. The relative difference between the variational and numerical binding energies are shown in Figs. 3(a)–3(c), and we see that the agreement is extremely good. The highest discrepancy of some

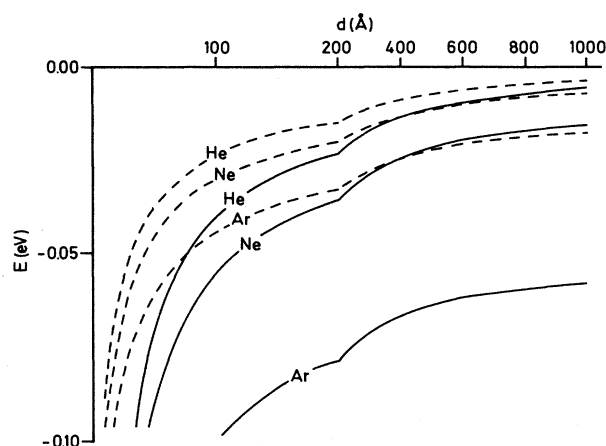


FIG. 2. Variational binding energies as functions of the layer thickness d , for He, Ne, and Ar: ground states (solid lines) and first excited states (dashed lines) are shown. The limiting values are $E_i = -Z^2 0.85 / (i+1)$ ($i=0,1$).

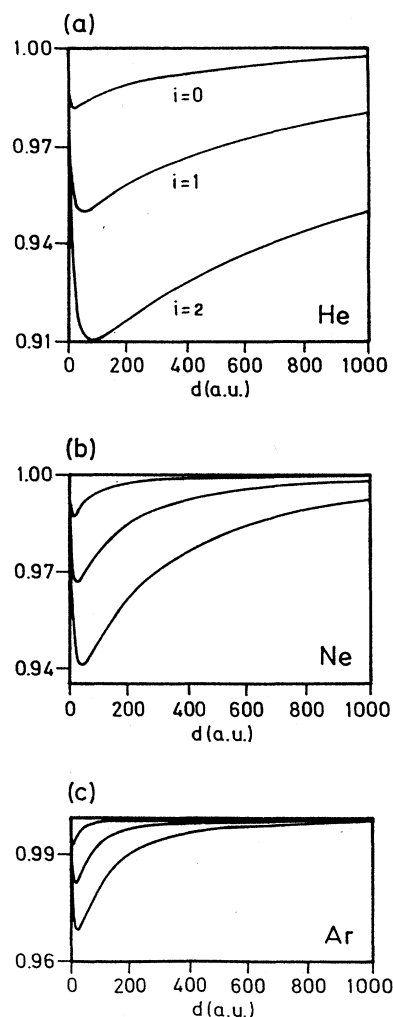


FIG. 3. Ratios of the variational and numerical energies of the first three image-potential states as functions of (a) helium, (b) neon, and (c) argon, for layer thickness d .

10% arises for the second excited state on a helium layer of thickness 30–200 a.u., but, e.g., for the ground state, they are practically negligible. The agreement is better for lower states and for larger dielectric constants ϵ_0 , as can be seen in Fig. 3, e.g., comparing the helium and argon cases.

The main motivation for this variational approach was to find the approximate wave functions in a simple form, which could be used in further studies of these quasi-two-dimensional systems.⁹ The real test of the validity of the variational approach is not only the eigenenergies, but especially the electronic wave functions.

In Fig. 4 we show that the ground-state wave functions are extremely well given by the variational form (10) with α 's calculated for Ne at two different thicknesses, even in the region of highest discrepancy ($d = 50$ and 200 a.u.)

The ground state is particularly well approximated, and we find certain deviations for higher excited states, as expected. As a typical quantity to compare, we might take the first moment (or average distance from the surface) of the electron density—namely, these states characteristically extend rather far into the vacuum. Figure 5 shows variationally calculated average distances \bar{z} for the three lowest states of He, Ar, and Ne—with increasing thickness d they gradually approach the bulk dielectric results. This figure also gives the parameters $\alpha_0(d)$ for the three gases. Figure 6 again confirms the quality of our variational wave functions: the deviations from the numerically computed values of \bar{z} are indeed very small.

Finally, in Fig. 7 we compare our numerical results with those of Cole⁸ and find excellent agreement regardless of the different expressions for image potentials; namely, Cole introduced a cutoff of the image potential close to the surface and a finite barrier.

In conclusion, we have presented relatively simple analytic forms of the wave functions for the three lowest image-potential states trapped on the surfaces of dielectric layers on a metallic substrate, which are in excellent agreement with much more complicated numerical results. We have also given explicit results for the varia-

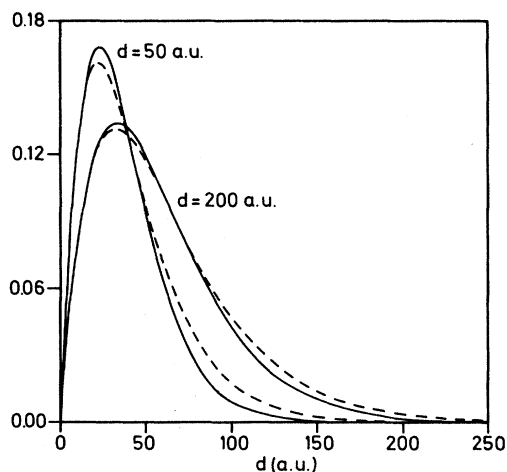


FIG. 4. The ground-state variational (dashed lines) and numerical (solid lines) wave functions of Ne at thicknesses of 50 and 200 a.u.

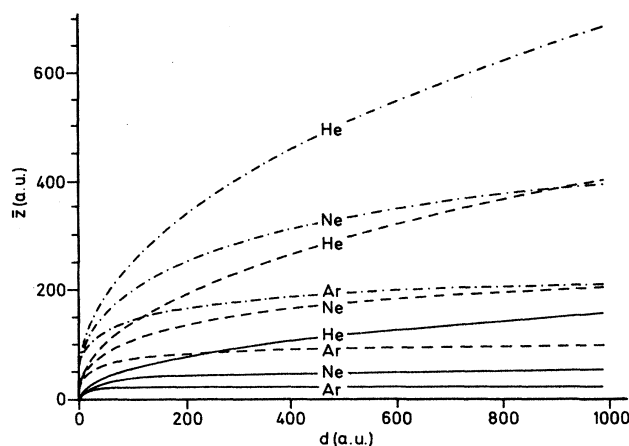


FIG. 5. The mean values \bar{z} for the ground (solid lines), first excited (dashed lines), and second excited states (dashed-dotted lines) of He, Ne, and Ar.

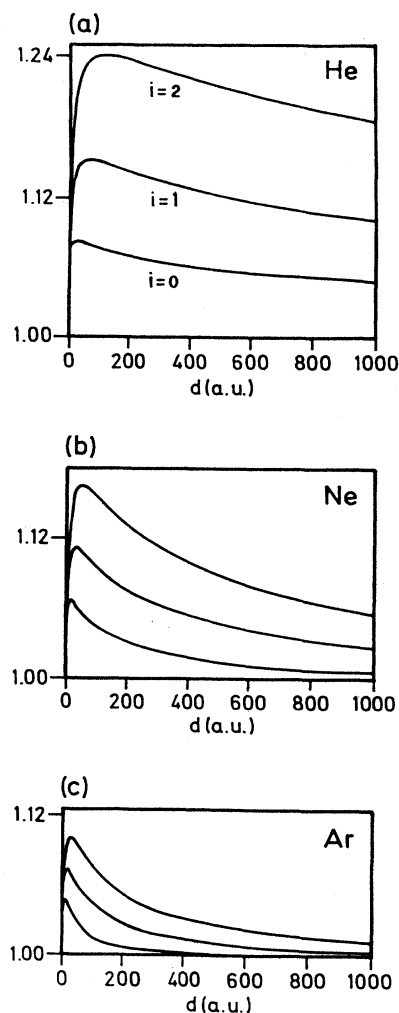


FIG. 6. The ratios of variationally numerically calculated average distances \bar{z} of the three lowest states as functions of (a) He, (b) Ne, and (c) Ar for layer thicknesses d .

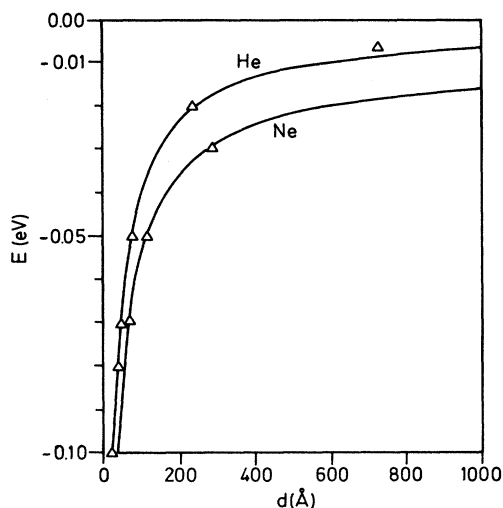


FIG. 7. Numerically calculated ground-state energies for helium and neon. Solid lines are our results, as compared with those of Ref. 8, denoted by triangles.

tional parameters appropriate to the layers of He, Ar, and Ne with varying thicknesses. The presented results enabled us to proceed with analytic modeling of quasi-two-dimensional electrons in such systems, which show a range of interesting phenomena.⁹

At present we are not aware of any systematic experimental study of these states, except for very thin dielectric films with several layers of thickness.

ACKNOWLEDGMENTS

This work was partially supported by the United States-Yugoslav Joint Board on Scientific and Technological Cooperation through Grant No. JFP-695/NBS.

APPENDIX

In this Appendix we give the relations between the coefficients a_i, b_i and the parameters α_i of the trial functions (10). We also give the average values of the Hamiltonian (12), $E_i = \langle \psi_i | H | \psi_i \rangle$, and the mean values of z :

$$\bar{z}_i = \int_0^\infty \psi_i z \psi_i dz. \quad (\text{A1})$$

$$\frac{1}{12} + \frac{\alpha_1^2}{\Lambda_1} \left[1 + \frac{\alpha_1(\alpha_0 - \alpha_1)}{2\Lambda_1} \right] = \int_0^\infty \frac{x dx}{(1+x)^6} \left[\frac{5}{\alpha_1} + \frac{3\alpha_1(1+x)}{\Lambda_1} + \frac{3\Lambda_2}{\Lambda_1} \left[5x + \frac{2\alpha_1(\alpha_0 - \alpha_1)(1+x)}{\Lambda_1} \right] \right] \frac{\beta + e^{-xD\alpha_1/4}}{1 + \beta e^{-xD\alpha_1/4}}. \quad (\text{A7})$$

The mean value of z (in a.u.) is

$$\bar{z}_1 = \frac{4}{\alpha_1} \frac{20\alpha_0^2 - 4\alpha_0\alpha_1 + 2\alpha_1^2}{\Lambda_1}. \quad (\text{A8})$$

The analogous results for the second excited state are too lengthy to be given here.

Ground state

The average energy (in Ry) is

$$E_0(\alpha_0, d) = \frac{\alpha_0^2}{16} - \frac{\alpha_0}{4} \int_0^\infty \frac{dx}{(1+x)^3} \frac{\beta + e^{-xD\alpha_0/2}}{1 + \beta e^{-xD\alpha_0/2}}, \quad (\text{A2})$$

where $D = d/a_0$.

Minimizing the energy with respect to the parameter α_0 , we find that α_0 is given by the implicit equation

$$\alpha_0 = 6 \int_0^\infty \frac{x dx}{(1+x)^4} \frac{\beta + e^{-xD\alpha_0/2}}{1 + \beta e^{-xD\alpha_0/2}}. \quad (\text{A3})$$

The mean value \bar{z}_0 (in a.u.) is

$$\bar{z}_0 = \frac{6}{\alpha_0}. \quad (\text{A4})$$

First excited state

The orthonormalization conditions connect the coefficients in the trial function ψ_1 :

$$a_1^2 = \frac{3\alpha_1^2}{\Lambda_1}, \quad a_2 = -\frac{a_1}{24} \left[1 + \frac{2\alpha_0}{\alpha_1} \right], \quad (\text{A5})$$

where

$$\Lambda_1 = 4\alpha_0^2 - 2\alpha_0\alpha_1 + \alpha_1^2.$$

The average value E_1 (in Ry) is

$$E_1(\alpha_0, \alpha_1, d) = \frac{1}{8} \left[\frac{\alpha_1^2}{24} \left[1 + \frac{6\alpha_1^2}{\Lambda_1} \right] - \alpha_1 \int_0^\infty \frac{dx}{(1+x)^5} \left[1 + \frac{3\alpha_1 x \Lambda_2}{\Lambda_1} \right] \times \frac{\beta + e^{-xD\alpha_1/4}}{1 + \beta e^{-xD\alpha_1/4}} \right], \quad (\text{A6})$$

where

$$\Lambda_2 = -2\alpha_0 + \alpha_1 + \alpha_1 x.$$

α_1 is the solution of the equation

- *Present and permanent address: Faculty of Mining, Geology and Petroleum Engineering, University of Zagreb, P.O. Box 186, 41001 Zagreb, Croatia, Yugoslavia.
- ¹V. Dose, *Surf. Sci. Rep.* **5**, 337 (1985).
- ²P. D. Johnson, and N. V. Smith, *Phys. Rev. B* **27**, 2527 (1983).
- ³N. V. Smith and P. D. Woodruff, *Prog. Surf. Sci.* **21**, 295 (1986).
- ⁴M. W. Cole and M. H. Cohen, *Phys. Rev. Lett.* **23**, 1238 (1969); V. B. Shikin, *Zh. Eksp. Teor. Fiz.* **58**, 1748 (1970) [*Sov. Phys.—JETP* **31**, 936 (1970)].
- ⁵C. C. Grimes and T. R. Brown, *Phys. Rev. Lett.* **23**, 280 (1974).
- ⁶K. H. Frank, K. Horn, J. Wilder, and E. E. Koch, *Appl. Phys. A* **44**, 330 (1987).
- ⁷K. Wandelt, W. Jacob, N. Memmel, and V. Dose, *Phys. Rev. Lett.* **57**, 1643 (1986).
- ⁸M. V. Cole, *Phys. Rev. B* **3**, 4418 (1971).
- ⁹M. Šunjić and Z. Lenac (unpublished).
- ¹⁰Z. Lenac and M. Šunjić (unpublished).
- ¹¹Z. Penzar and M. Šunjić, *Phys. Scr.* **30**, 431 (1984).
- ¹²Z. Lenac, M.Sc. thesis, University of Zagreb, 1980.
- ¹³M. L. Klein and J. A. Venables, *Rare Gas Solids* (Academic, New York, 1976), Vol. II, Chap. 17.
- ¹⁴N. Schwentner, M. Skibowski, and W. Steinmann, *Phys. Rev. B* **8**, 2965 (1973).
- ¹⁵V. Saile and E. E. Koch, *Phys. Rev. B* **20**, 784 (1979).
- ¹⁶N. Schwentner, F. J. Himpsel, V. Saile, M. Skibowski, W. Steinmann, and E. E. Koch, *Phys. Rev. Lett.* **34**, 528 (1979).